

## An Enhanced Influence of Tropical Indian Ocean on the South Asia High after the Late 1970s

XIA QU

*Center for Monsoon System Research, Institute of Atmospheric Physics, Chinese Academy of Sciences, Beijing, and Key Laboratory of Global Change and Marine-Atmospheric Chemistry, Third Institute of Oceanography, State Oceanic Administration, Xiamen, China*

GANG HUANG

*Key Laboratory of Regional Climate-Environment Research for Temperate East Asia, Institute of Atmospheric Physics, Chinese Academy of Sciences, Beijing, China*

(Manuscript received 29 November 2011, in final form 9 April 2012)

### ABSTRACT

The tropical Indian Ocean (TIO)'s influence on the South Asia high (SAH)'s intensity experiences a decadal change in the late 1970s; after (before) the decadal shift, the influence is significant (insignificant). The present study investigates the role of tropospheric temperature in relaying the impact of sea surface temperature (SST) to the SAH and the change in the TIO's influence. During the two epochs, the local tropospheric temperature responses to the TIO warming are distinct—more significant during the second epoch. It is inferred that this change may be responsible for the strengthening of the TIO's influence on the SAH. Encouragingly, the ensemble simulations accurately capture the time of the decadal change, indicating that the enhanced influence is attributed to the SST forcing.

There are two possible reasons for the change in the TIO–SAH relationship. The first reason is the change in the locations of the SST anomalies in the TIO. During the second epoch, positive SST anomalies lie in the Indian Ocean warm pool. Through the background vigorous convection and moist adjustment, the SST anomalies affect largely the tropospheric temperature and thus the SAH. The second reason is the decadal change in mean SST and the SST variability. During the recent decades, both the background SST and the variability of the TIO SST increase, which enhance the influence of the SST anomalies on the atmosphere. The influence of the remote oceanic forcing on the enhanced TIO–SAH relationship and its comparison with the contribution of the TIO SST are also discussed.

### 1. Introduction

In boreal summer, there exists a high pressure system in the upper troposphere and the lower stratosphere (UTLS) over the Tibetan Plateau and the surrounding area (Fig. 1). This high pressure system, called the South Asia high (SAH) or the South Asian anticyclone, forms due to the elevated heating of the Tibetan Plateau and the latent heating of the South Asian monsoon (Flohn 1960; Hoskins and Rodwell 1995; Duan and Wu 2005; Boos and Kuang 2010). The SAH is the strongest and steadiest system in the upper troposphere (Mason and

Anderson 1963; Li et al. 2005). The SAH influences the distribution of several trace constituents and pollution in the UTLS. The tropical and subtropical jets, residing on the south and north flanks of the SAH, form a barrier for meridional transports of some constituents, such as water vapor and ozone (Dethof et al. 1999; Randel and Park 2006). As a consequence, carbon monoxide (CO), after being transported from the lower troposphere to the UTLS, is trapped in the center of the SAH, leading to the maximum concentration there (Park et al. 2004; Li et al. 2005).

East Asia is one of the most highly populated regions. Severe floods and droughts, induced by the strong interannual variability of the East Asia summer monsoon (Huang et al. 1999), exert a large societal and economic influence. Studies showed that the East Asian summer monsoon rainfall is closely related to the western Pacific

---

*Corresponding author address:* Dr. Gang Huang, RCE-TEA, Institute of Atmospheric Physics, Chinese Academy of Sciences, P.O. Box 9804, Beijing 100029, China.  
E-mail: hg@mail.iap.ac.cn

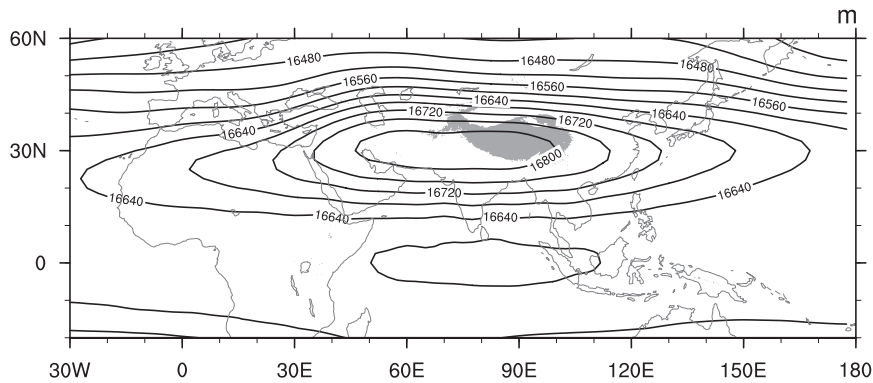


FIG. 1. June–August mean 100-hPa geopotential height for 1964–95; the contour interval is 40 m. Topography >3000 m is shaded.

subtropical high (WPSH; Tao and Chen 1987; Huang and Wu 1989; Huang and Sun 1992; Wu and Chen 1998), whereas the variation of the WPSH follows that of the SAH (Tao and Zhu 1964; Jiang et al. 2011). In year-to-year variations, the intensified SAH, through emanating anomalous wave energy downstream, leads to the strengthening of the WPSH (Zhao et al. 2009). In turn, this results in the decrease of rainfall over the western North Pacific (WNP) and the increase of rainfall over East Asia (Zhang et al. 2005; Zhao et al. 2007). In addition, studies suggested that the interannual variability of the SAH is associated with the South Asia monsoon, the mid-Pacific trough, and the Mexico high (Zhang et al. 2005; Zhao et al. 2007).

Previous studies found that the interannual variability of the SAH is tightly linked to the tropical Indian Ocean (TIO) sea surface temperature (SST; Zhang et al. 2000; Yang et al. 2007; Yang and Liu 2008; Huang et al. 2011). The influence of the TIO SST has been overlooked in earlier years because the interannual variability of the TIO SST is relatively small. Recent studies indicate that the TIO SST exerts influences on climate when the SST anomalies in the other oceans are relatively small. In boreal summer, the temperature in most parts of the eastern or central Indian Ocean is greater than 28°C. Because of the nonlinearity of the Clausius–Clapeyron equation, a small change in the Indian Ocean SST may have a large impact on moisture availability as well as tropical convection (Zhang 1993). On interannual time scale, the TIO warms up following the peak of El Niño through “atmospheric bridge” and oceanic dynamics (Klein et al. 1999; Xie et al. 2002). This warming persists to summer, when El Niño has dissipated, and exerts influences on summer climate (Annamalai et al. 2005; Yang et al. 2007; Xie et al. 2009). The process is like charging and recharging, called “capacitor effect.” The persistent warming in summer, through convection and moist

adjustment, heats the whole tropospheric column, forces the Kelvin wave to the east and affects the WNP climate (Xie et al. 2009) and the East Asia climate (Hu et al. 2011a,b). The warmed tropospheric column over the TIO corresponds to an elevation of the geopotential height in the upper troposphere and leads to an anomalous SAH (Huang et al. 2011).

Furthermore, recent studies found that owing to the thermocline shoaling and the strengthened variability of El Niño–Southern Oscillation, the TIO’s influences on WNP climate intensified after the late 1970s (Huang et al. 2010; Xie et al. 2010). However, it is still unknown whether similar decadal change exists in the TIO’s influences on the SAH. The aim of the present study is to investigate the decadal change in the TIO’s influences on the SAH and the possible causes.

The article is organized as follows: section 2 is the introduction of data and methods; section 3 presents the observational results; section 4 shows the AGCM [ECHAM5 and Community Atmosphere Model, version 3 (CAM3)] results; section 5 gives the two possible reasons leading to the decadal change; section 6 discusses the effect of the remote oceanic forcing and the time of the decadal change; and section 7 summarizes the founding.

## 2. Data and methods

### a. Observations

The datasets used in the present study include 1) the Met Office Hadley Centre Sea Ice and Sea Surface Temperature (HadISST) dataset (Rayner et al. 2006) and 2) the National Centers for Environmental Prediction–National Center for Atmosphere Research (NCEP–NCAR) atmospheric reanalysis dataset (Kalnay et al. 1996). The horizontal resolutions of these datasets

are  $1^\circ \times 1^\circ$  and  $2.5^\circ \times 2.5^\circ$ , respectively. The analysis and discussion in this paper focus on the period 1959–2000.

The present study is concerned with the interannual variability and its decadal change. Since significant trend has been found in both the TIO SST and SAH (Zhang et al. 2000; Du and Xie 2008), the data have been detrended to eliminate the contribution of longer time-scale variations to the statistical results. The detrending is performed on the data of each period. For instance, if the target period of analysis is from 1964 to 1979, then the trend for the period 1964–79 is removed before the analysis. In this study, summer refers to the period from June to August.

In this study, the TIO SST index is defined using the area average of SST in the domain ( $20^\circ\text{S}$ – $20^\circ\text{N}$ ,  $40^\circ$ – $100^\circ\text{E}$ ) with latitudinal weight, following Xie et al. (2009) and Huang et al. (2010). The SAH intensity index, which is the same as that in Zhang et al. (2000) and Zhou et al. (2006), is defined as the sum of differences between a reference height (16 600 m) and the geopotential height at each point where the geopotential height is no less than 16 600 m in the region ( $10^\circ\text{S}$ – $50^\circ\text{N}$ ,  $30^\circ\text{W}$ – $180^\circ\text{E}$ ).

### b. Atmospheric simulations

To understand the contribution of the SST change to the observed decadal shift of the TIO's influences on SAH, two atmospheric general circulation models (AGCMs) are employed: the Hamburg version of the European Centre for Medium-Range Weather Forecasts model, version 5 (ECHAM5; Roeckner et al. 2003) and CAM3 (Collins et al. 2004). The resolutions of the two AGCMs are T63L19 and T42L26, respectively. The AGCMs are driven by global historical SST and sea ice. A 17-member ensemble simulation is conducted for 1950–2007 with ECHAM5 and a 21-member ensemble simulation for 1950–99 with CAM3. The ensemble means are used in the analysis (unless stated) to exclude the internal variability of the AGCMs and the error due to initial condition.

To compare the relative impacts of the northern Indian Ocean (NIO) SST and the southern Indian Ocean (SIO) SST, we have performed three experiments with ECHAM5. In the control (CTL) experiment (40 integrations), the AGCM is driven by climatological SST. In the NIO experiment (20 integrations), a  $1^\circ\text{C}$  SST anomaly (SSTA) is imposed on the climatological SST in the domain ( $0^\circ$ – $20^\circ\text{N}$ ,  $40^\circ$ – $100^\circ\text{E}$ ). The SIO experiment is the same as the NIO experiment, except that the domain for the SST anomaly is  $20^\circ\text{S}$ – $0^\circ$ ,  $40^\circ$ – $100^\circ\text{E}$ . The difference between the NIO and CTL experiments is considered as the response to the northern Indian Ocean warming. The response of the southern Indian Ocean warming is represented by the difference between the SIO and CTL experiments.

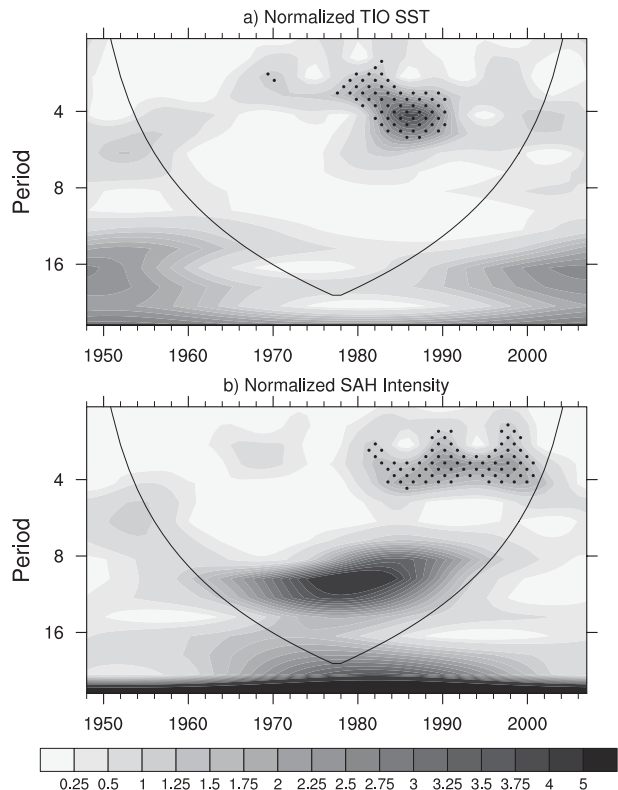


FIG. 2. Wavelet spectra of (a) normalized TIO SST and (b) normalized SAH intensity. Dots represent areas where the significance level reaches 95%. The results are obtained from raw data without detrending.

In addition, two AGCM experiments are designed: 1) the Indian Ocean climatological SST experiment (IOC) and 2) the Indian Ocean real SST experiment (IOR). The IOC is used to test the impacts of the remote oceanic forcing. In this experiment, climatological SST is used in the Indian Ocean. In other oceans, historical SST is adopted. The prescribed SST is used to drive ECHAM5. Only a single run is conducted for this experiment due to the time-consuming ensemble experiments. The IOR is used to test the influences of the Indian Ocean. It is the same as IOC but for historical SST in the Indian Ocean and climatological SST in other oceans.

### 3. The decadal change of the TIO–SAH relationship

The variability of both the TIO SST and SAH experiences a shift in the late 1970s. Figure 2 shows the wavelet spectra of normalized summertime TIO SST and SAH intensity. The TIO SST features a quasi-biennial variation from the mid-1960s to the late 1970s and a 4-yr period variation after the late 1970s. The SAH

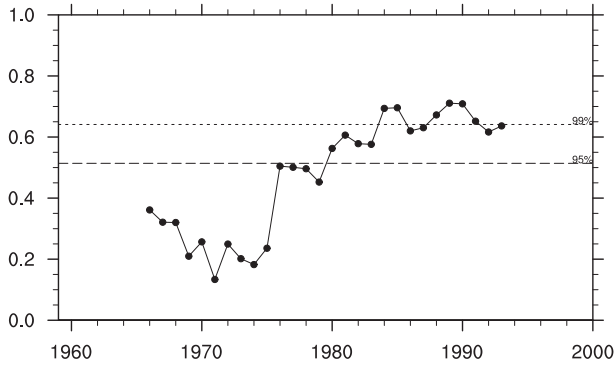


FIG. 3. The 15-yr sliding correlation between the TIO SST and the SAH intensity. Dashed and dotted lines represent the 95% and 99% significance levels, respectively. Both of the indices are undetrended.

index displays a tendency of a 4-yr period variation after the late 1970s, which is similar to the TIO SST. Different from the TIO SST, the quasi-biennial variation of the SAH is less significant before the late 1970s. In addition,

the SAH intensity features a distinct 10-yr period variation, which is not seen in the TIO SST.

The above change in the coherence of spectrum indicates that the association between the variability of the TIO SST and SAH may experience a strengthening at the late 1970s. This is confirmed by the 15-yr sliding correlation in Fig. 3. The correlation between the TIO SST and SAH experiences a shift around 1979; before 1979, the correlation is weak; after 1979, the correlation became significant, with the correlation coefficient (CC) reaching the 95% confidence level.

Previous studies show that the moist adjustment-induced tropospheric temperature changes play an important role in the TIO's influences on the SAH (Huang et al. 2011). To understand the change in the relationship between the TIO SST and the SAH, we contrast the response of tropospheric temperature to the TIO SST before and after the late 1970s. In the following analysis, we select 1964–79 for the period before the change and 1980–95 for the period after the change. For convenience,

### SST & Tropospheric Temperature

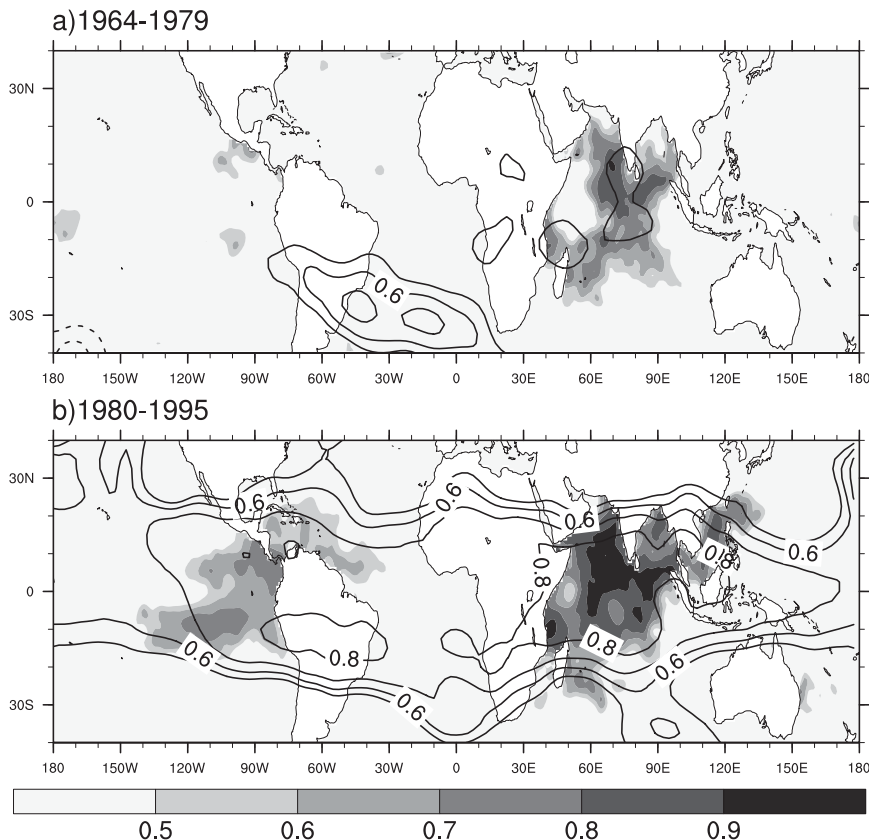


FIG. 4. Correlation of the TIO SST with SST (shading) and tropospheric temperature (contours), showing the results for (a) 1964–79 and (b) 1980–95. Only shading for 0.5, 0.6, 0.7, 0.8, and 0.9, and contours for  $\pm 0.5$ ,  $\pm 0.6$ ,  $\pm 0.7$ ,  $\pm 0.8$ , and  $\pm 0.9$  are displayed. Nine-point spatial smoothing is performed on the results.

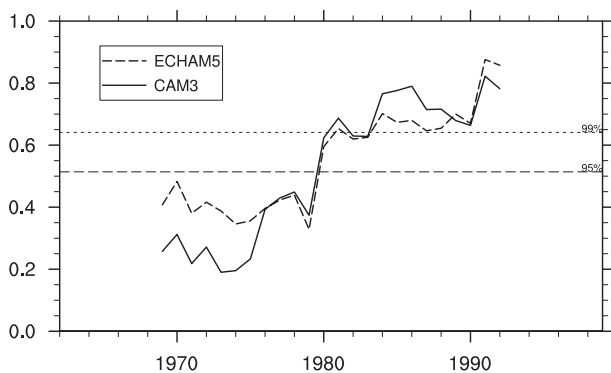


FIG. 5. Ensemble mean of 15-yr sliding correlation between the TIO SST and SAH intensity. Dashed and solid lines represent ECHAM5 and CAM3 results, respectively. Dashed and dotted lines denote the 95% and 99% significance levels, respectively.

the two epochs are called PRE and POST. Figure 4 shows the correlation of tropospheric temperature with the TIO SST during the two epochs. Like Huang et al. (2011), the tropospheric temperature is the average of the temperature from 850 to 100 hPa. During PRE, weak tropospheric temperature responses are observed over the central Indian Ocean and north of Madagascar. A significant response is also seen over subtropical South America and the South Atlantic. During POST, as the TIO warms, significant tropospheric warming is distributed over the global tropics. To the east of the equatorial Indian Ocean, the warm anomaly displays a Kelvin wavelike response, which may further affect the northwestern Pacific climate through boundary friction and convection–divergence feedback (Xie et al. 2009). To the west of the Indian Ocean, the tropospheric temperature shows a Rossby wavelike pattern, with two maximums off the equator. The Kelvin and Rossby wavelike patterns display the Matsuno–Gill (Matsuno 1966; Gill 1980) pattern, indicating they are the responses to Indian Ocean heating. The CCs are most significant over the TIO ( $CC > 0.8$ ). This implies that through moist adjustment, the TIO SST can significantly affect the tropospheric temperature, resulting in anomalies in 100-hPa geopotential height and leading to the change in the SAH. Therefore, the relationship between the TIO SST and the SAH is closer during POST than during PRE.

To test the hypothesis that the strengthening of the TIO–SAH relationship is attributed to the SST forcing, we further analyzed the results of AGCM simulations.

#### 4. The shift in AGCMs simulations

To examine whether the SST change contributes to the intensification of the TIO's influence on the SAH, we analyze the results of AGCM simulations. In view of the systematic difference of mean 100-hPa geopotential height between ECHAM5 and the NCEP–NCAR reanalysis,

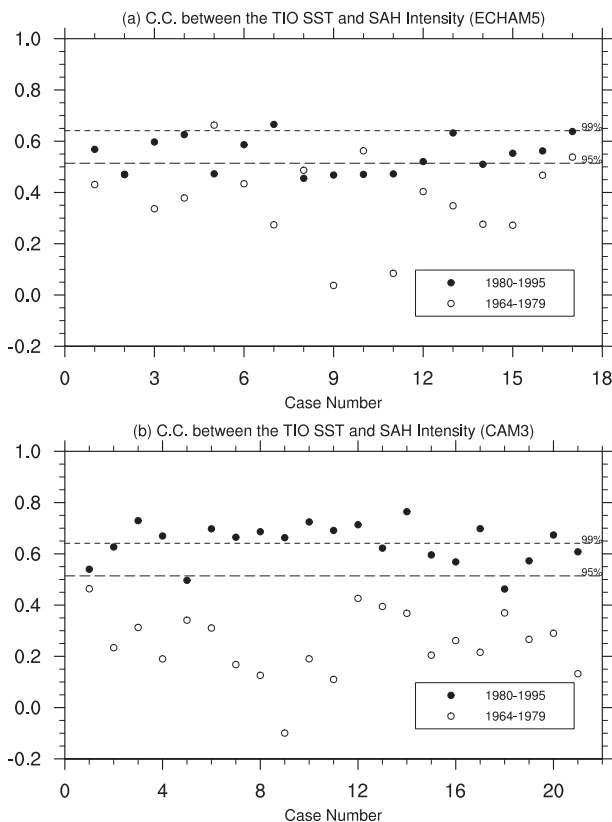


FIG. 6. CCs between the TIO SST and SAH intensity, with the results of (a) ECHAM5 and (b) CAM3. Circles denote the results for 1964–79, and dots denote the results for 1980–95. Case tabs are on the x axis, and the CCs are on the y axis.

a somewhat different reference height (16 860 m) is used in defining the SAH intensity for the ECHAM5, following Huang et al. (2011). For CAM3, the mean difference from the reanalysis is very small, so the definition of the SAH intensity is the same as Zhang et al. (2000) and Zhou et al. (2006).

Both the ECHAM5 and CAM3 simulations reproduce well the intensification of the TIO SST–SAH relationship at the late 1970s. Figure 5 displays the 15-yr sliding correlation between the TIO SST and SAH intensity calculated based on the ensemble mean. During PRE, the model simulations exhibit weak TIO–SAH correlation ( $CCs < 0.5$ ). Around 1979, the correlation experiences an obvious increase ( $CCs > 0.6$ ). The ensemble mean CCs between the TIO SST and SAH intensity during PRE and POST are 0.39 (0.25) and 0.64 (0.64), respectively, in ECHAM5 (CAM3), which are in agreement with those in observation. Therefore, the model results suggest the importance of SST forcing in the strengthening of the TIO–SAH relationship.

We have also calculated the correlation for individual members. Most of the simulations can reproduce the

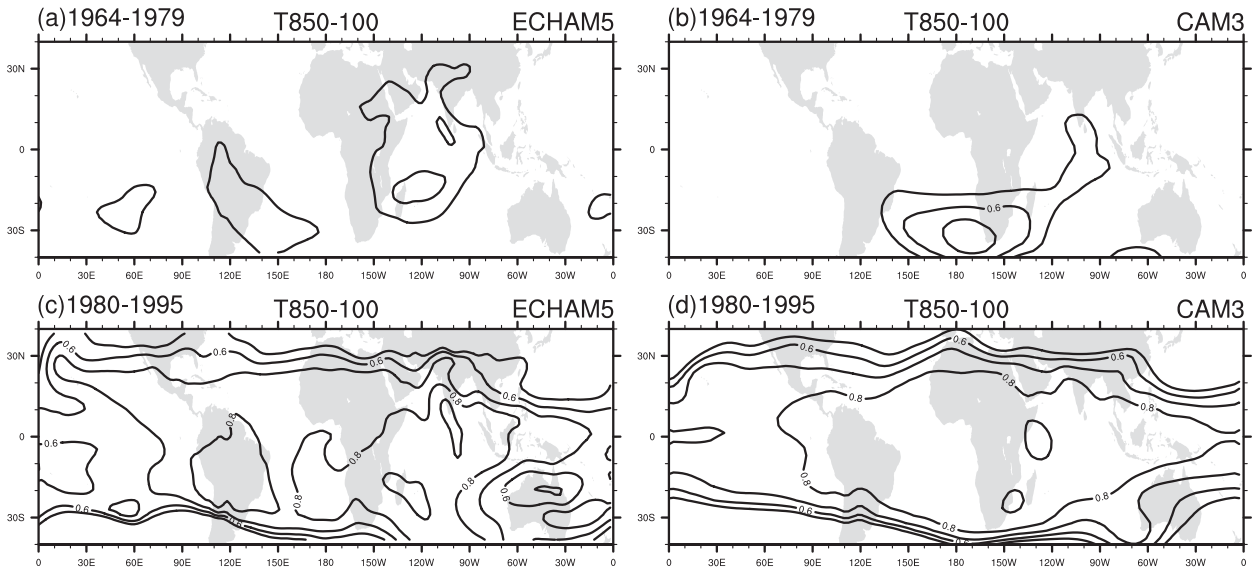


FIG. 7. Correlation of the TIO SST with tropospheric temperature, showing the results for (a),(b) 1964–79 and (c),(d) 1980–95 with the results of (a),(c) ECHAM5 and (b),(d) CAM3. Only shading and contours for  $\pm 0.5$ ,  $\pm 0.6$ ,  $\pm 0.7$ ,  $\pm 0.8$ , and  $\pm 0.9$  are displayed. Nine-point spatial smoothing is performed on the results.

intensification of the TIO–SAH relationship. Figure 6 shows the CCs of each simulation during PRE and POST. In ECHAM5, 13 out of 17 cases can reproduce the strengthening of the TIO–SAH relationship (Fig. 6a). In the remaining four cases, the CCs of PRE are greater than those of POST in cases 4, 8, and 10. In case 2, there is nearly no difference in the CCs between PRE and POST. These may be attributed to the initial condition and model internal variability. All the CAM3 simulations reproduce the intensification of the TIO–SAH relationship (Fig. 6b). In this aspect, CAM3 presents more realistic outputs than ECHAM5.

Both ECHAM5 and CAM3 ensemble means can reproduce well the tropospheric temperature responses to the TIO warming. Figures 7a and 7c display the correlation of tropospheric temperature with the TIO SST in ECHAM5. Figures 7b and 7d are the same, except for CAM3. During PRE, when the TIO warms, a weak tropospheric temperature response exists over part of the Indian Ocean and east of Africa. So, the TIO–SAH relationship during this period is weak. During POST, as the TIO warms, a tropospheric temperature anomaly is distributed over the global tropics. The tropospheric temperature response is similar to that in observation. To the east of the TIO, the Kelvin wave response is also reproduced. Overall, the ECHAM5 and CAM3 simulations reproduce well the tropospheric temperature anomalies in response to the TIO warming, which can in turn lead to the change in upper-level geopotential height and the SAH.

In these two AGCMs, the overall response, including the tropospheric temperature and the SAH, is slightly

exaggerated compared with that in observation. This may be caused by the removal of internal variability due to ensemble mean. Besides this subtle difference, the ensemble results of the two AGCMs can well reproduce the strengthening of the TIO–SAH relationship and the responses of the tropospheric temperature during the two epochs. This suggests that the strengthening of the TIO–SAH relationship is caused by the decadal change in SST forcing.

## 5. Possible mechanisms

The model simulations in the previous section indicate the contribution of the SST forcing to the decadal change in the TIO SST–SAH relationship. The SST forcing includes the TIO local forcing and the remote oceanic forcing (the latter one is discussed in the next section). To remove the effect of the remote oceanic forcing (the influences of ENSO), the partial correlation analysis is performed during the two epochs. The partial correlation is calculated using

$$r_{13,2} = \frac{r_{13} - r_{23}r_{12}}{\sqrt{1 - r_{23}^2}\sqrt{1 - r_{12}^2}}, \quad (1)$$

where the  $r_{13,2}$  denotes the CC between 1 and 3 by removing the impact of 2,  $r_{13}$  denotes the CC between 1 and 3,  $r_{23}$  denotes the CC between 2 and 3, and  $r_{12}$  denotes the CC between 1 and 2. After removing the influences of ENSO measured by the November (0)–January (1) Niño-3.4 SST index (numerals “0” and “1” denote the previous

year and this year, respectively), the CC between the TIO SST and the SAH is  $-0.05$  during PRE and  $0.52$  during POST. It suggests that the decadal change exists regardless of the remote oceanic forcing, especially the influences of ENSO.

The rest of this section discusses the possible mechanisms, including the location of the TIO SST anomalies and the change of the SST variability.

#### a. The locations of SST anomalies in the TIO

Tropical convection can modulate the tropospheric temperature toward a moist-adiabatic profile, which is determined by an equivalent potential temperature in the atmospheric boundary layer (Emanuel et al. 1994, 1997). In this process, convection acts as a key role of communicating SST with the tropospheric temperature (Chiang and Sobel 2002): If the tropospheric temperature is lower than the moist-adiabatic profile, then the atmosphere is unstable. Convective precipitation will occur and the associated latent heat release will adjust the tropospheric temperature toward the moist-adiabatic profile. If there is no convection, then the SST and tropospheric temperature cannot be well coupled, since the modulating mechanism does not exist. As deep convection exists only over the central and northeastern Indian Ocean, the location of SSTAs may determine their influences on tropospheric temperature. Thus, we first focus on the change in the location of SST anomalies and its consequence on the atmosphere responses.

Figure 8 shows the regression map of SST and surface wind (10 m) against the TIO SST for PRE and POST, respectively. The climatological mean SST is superposed on the map. Compared with PRE, the climatological mean SST during POST is about  $0.5^{\circ}\text{C}$  warmer, which leads to a slight westward extension of the Indian Ocean warm pool. During the two epochs, the SSTA distributions are different. During PRE, an obvious SSTA ( $>0.2^{\circ}\text{C}$ ) is found in the southeastern Indian Ocean, outside of the warm pool (Fig. 8a). The warm anomaly may be attributed to the deceleration of surface winds due to the superposition of the anomalous northerly (northeasterly) on the climatological southeasterly to the north of the Mascarene high. Over the southeastern Indian Ocean, outside of the warm pool, the climatological convection is relatively weak, and the SSTA cannot be well coupled with the tropospheric temperature. Thus, the above tropospheric warming is not significant (Figs. 4a, 7a, and 7b). Over the northern Indian Ocean, the anomalous surface easterly counteracts the climatological westerly, decelerates the actual wind, weakens the evaporation locally, and leads to the warm SST anomaly. The SST anomaly, however, is very weak ( $<0.2^{\circ}\text{C}$ ) and thus exerts little influence on the tropospheric temperature.

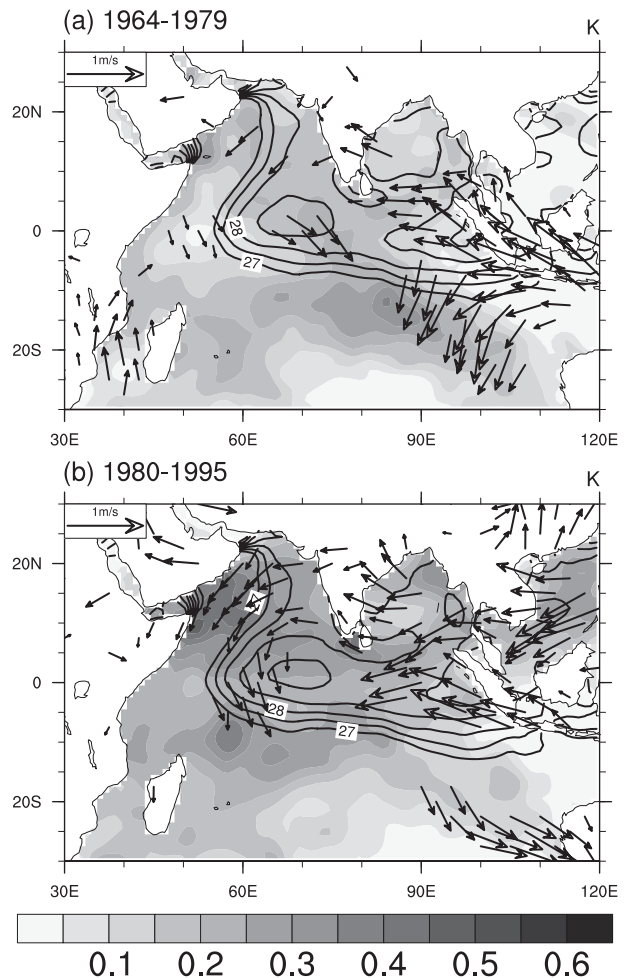


FIG. 8. Regression of SST (shading), surface wind (10 m, vectors) against the TIO SST and the mean SST in boreal summer, showing the results for (a) 1964–79 and (b) 1980–95. Nine-point spatial smoothing is performed on the regressed SST. Only vectors at the 95% significant level are shown.

During POST, the intensified variability of ENSO results in more significant ENSO-induced downwelling Rossby waves reaching the tropical southwestern Indian Ocean. The downwelling Rossby waves interact with the shallow thermocline there and lead to obvious ocean warming (Huang and Kinter 2002; Xie et al. 2002). In addition, the thermocline in the tropical southwestern Indian Ocean shoals relative to that during PRE. It locally results in more significant warming. The warming persists to summer and leads to a C-type wind anomaly over the TIO (the more significant anomalous easterly or northeasterly over the northern Indian Ocean). The anomalous wind counteracts the climatological wind, decelerates the actual wind, and leads to more significant warming over the northern Indian Ocean (Wu et al. 2008; Du et al. 2009; Wu and Yeh 2010). As the warming

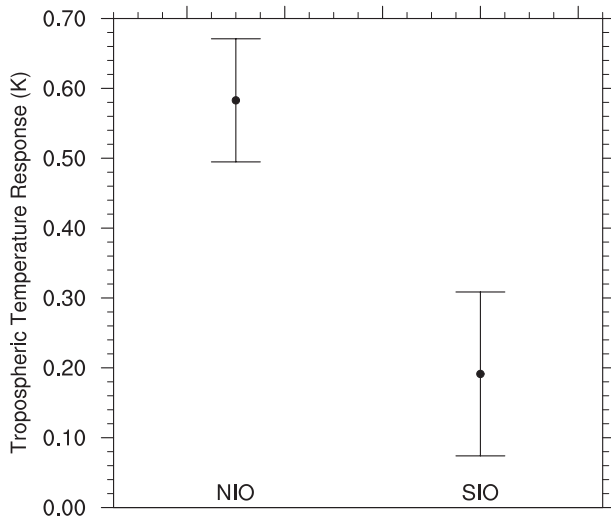


FIG. 9. Tropospheric temperature anomalies (dots) and standard deviations (the lengths between the end of each error line and the central dot) in (left) the NIO experiment and (right) the SIO experiment.

is mainly located in the warm pool, where the convection is vigorous, the warming can effectively affect the tropospheric temperature through moist adjustment (Figs. 4b, 7c, and 7d). Thus, the tropospheric temperature response is significant when the TIO is warming during POST.

The importance of the northern Indian Ocean SSTA is supported by results of sensitive experiments. As the northern Indian Ocean is  $1^{\circ}\text{C}$  warmer, the tropospheric temperature response is significant ( $0.58^{\circ}\text{C}$ ; Fig. 9). In contrast, the response to the southern Indian Ocean warming is only  $0.19^{\circ}\text{C}$ , which is far less than that to the northern Indian Ocean warming. Furthermore, in the SIO experiment, the spread is larger, indicating that the response is more uncertain. It can be inferred from the climatological SST in Fig. 8 that the climatological convection over the northern Indian Ocean is stronger than that over the southern Indian Ocean. With the background of strong convection, SSTAs over the northern Indian Ocean can effectively affect the overlying tropospheric temperature, confirming the more significant influence of the northern Indian Ocean SST.

#### b. The change of the SST variability in the TIO

After the 1960s, the TIO SST gradually increases. As such, the background SST during POST is warmer than that during PRE (Fig. 10). Meanwhile, the variability of the TIO SST during POST strengthens (Fig. 11). The standard deviation is  $0.19\text{ K}$  during PRE and  $0.24\text{ K}$  during POST. The combined effect of the change in the mean SST and the SST variability may be one of the

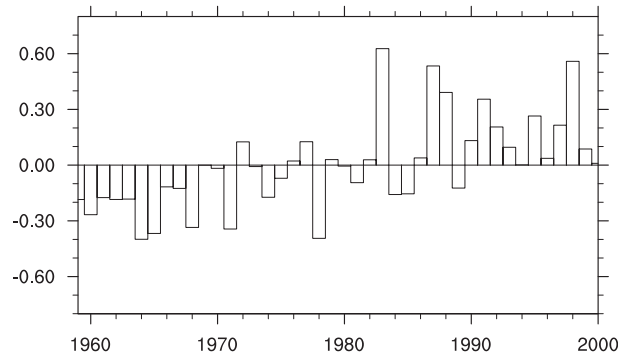


FIG. 10. Summertime TIO SSTA (without detrending, unit:  $^{\circ}\text{C}$ ).

possible reasons that lead to the strengthening of the TIO's influence on tropospheric temperature.

From the mid-1960s to the mid-1980s, the variability of the northern Indian Ocean and the southern Indian Ocean SST displays distinct characters (Fig. 11). The variability of the southern Indian Ocean SST shows a steady increasing trend. Before 1976, the standard deviation of the northern Indian Ocean SST is smaller than that of the southern Indian Ocean SST. The standard deviation of the northern Indian Ocean SST experienced an abrupt increase around 1976. After 1976, the standard deviation of the northern Indian Ocean SST is much larger than that of the southern Indian Ocean SST. From the temporal evolution of the SST standard deviation, it appears that the variability intensification of the TIO SST is mainly due to the strengthened variability of the northern Indian Ocean SST.

ENSO and the change in the thermocline depth of the tropical southwestern Indian Ocean play important roles on the change in the variability of the TIO SST. Long-term change in ENSO and the local thermocline results in more significant warming in the tropical southwestern

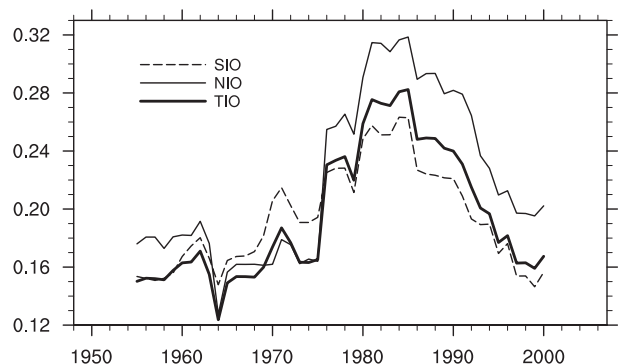


FIG. 11. The 15-yr sliding standard deviation (without detrending). Thick, thin, and dashed lines denote the results of the TIO SST, the NIO SST, and the SIO SST, respectively.

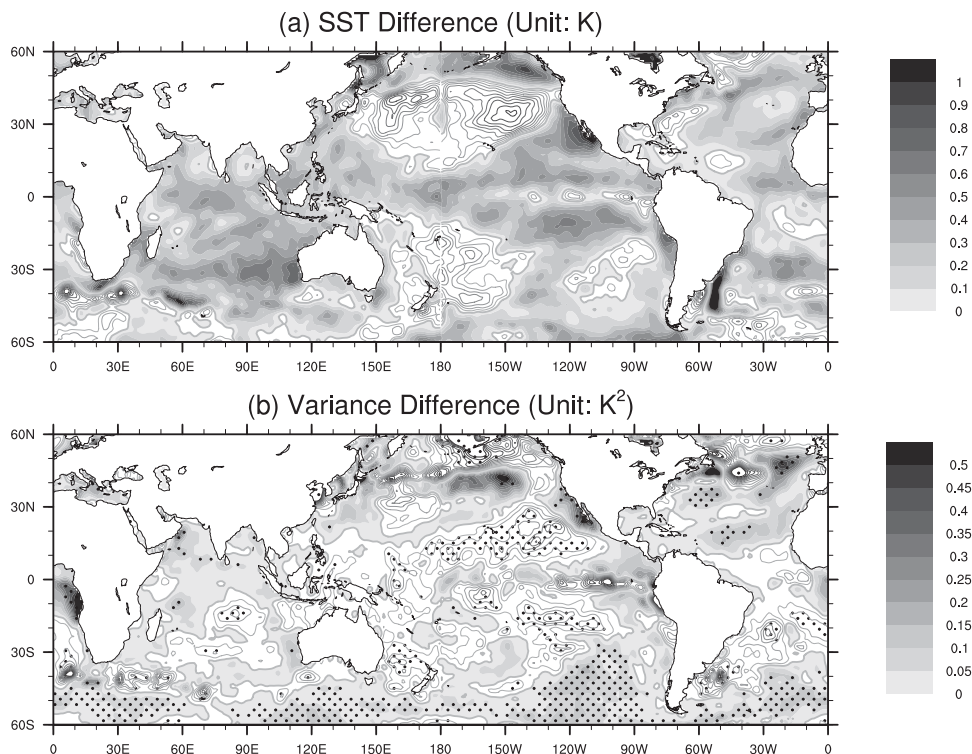


FIG. 12. Differences of (a) June–August mean SST and (b) its variance between 1980–95 and 1964–79. Shadings denote the differences greater than 0. Contours denote the differences not greater than 0; contours for 0 are thick. Interval of the shadings and contours is 0.1 K in (a) and 0.05 K<sup>2</sup> in (b). Dots in (b) denote the variance change is at the 90% significance level detected as by an  $F$  test. Nine-point spatial smoothing is performed on the results.

Indian Ocean in spring after the El Niño peaks (Xie et al. 2010). The warming excites anomalous C-type wind over the TIO (anomalous easterly or northeasterly over the northern Indian Ocean) and leads to the warming over the northern Indian Ocean (Wu et al. 2008; Du et al. 2009). Thus, nearly all basin warming is found in the Indian Ocean in summer. This contributes to the more significant variability of the TIO SST during POST. During PRE, the smaller standard deviation of ENSO and the deeper thermocline cause less warming over the southwestern Indian Ocean, and in turn less warming over the northern Indian Ocean. The TIO warming dissociates with ENSO and thus the SST variability of the TIO is relatively small during PRE.

However, it should be borne in mind that both the mean SST change and the variability change not only occur in the Indian Ocean but globally. Figure 12 gives the difference of the June–August mean SST and its variability. Besides the TIO, the northern Atlantic, the equatorial Atlantic to the west of Africa, and 40°–60°S of the southern oceans exhibit large-scale warming with increased SST variability during POST. Those may also exert influences on the atmosphere.

## 6. Discussion

### a. The remote oceanic forcing

When heated by eastern Pacific warming, the tropical free atmosphere cannot maintain a horizontal pressure gradient and the temperature anomalies become uniformly distributed over the global tropics on time scales of a month or two (Charney 1963; Wallace 1992; Sobel and Bretherton 2000). Interestingly, Chiang and Sobel (2002) suggested that not all the temperature anomalies (including those over the TIO) disappear 6 months after El Niño has peaks. That is to say, the free-atmosphere temperature is not only subject to local heating but also to the heating of the remote oceans. Here, the remote oceans' impacts on the intensification of the TIO's influences on the tropospheric temperature are discussed.

The effect of the remote oceanic forcing can be examined based on the IOC experiment. The CCs between the observed TIO SST and the simulated tropospheric temperature over the TIO in the IOC experiment are given in Fig. 13. During PRE, the CC is 0.21; the CC is 0.67 during POST. So, we can conclude that the remote oceans' influences on the tropospheric temperature also

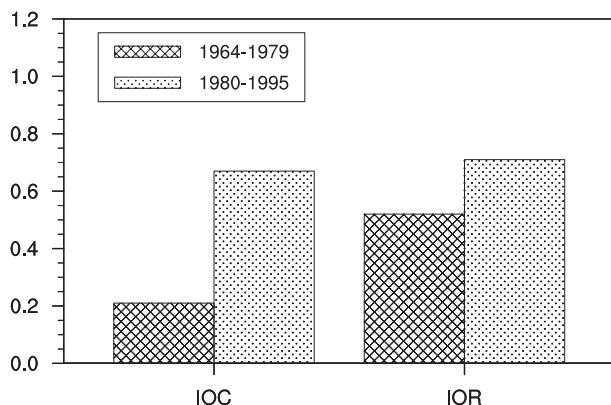


FIG. 13. Correlation between the observational TIO SST and the above tropospheric temperature in boreal summer, showing the results in the IOC (left two bars) and IOR experiments (right two bars). Bars with reticular stripes are the results for 1964–79, and those with dots are the results for 1980–95.

contribute to the strengthening of the TIO–SAH relationship.

In the decadal change in the remote oceans' influences, the SSTa over the eastern Pacific and Atlantic may be the main reason. During PRE, before the TIO basin warming, significant SSTAs are only found over the tropical eastern Pacific and near the date line (Fig. 14a). The areas of the SSTAs are scattered. During POST, the TIO SSTA is closely related to ENSO. The eastern Pacific shows significant warming starting in the previous summer (Fig. 14b). The warming persists to the previous autumn and winter and reaches its maximum. In the spring after it has peaks, the anomalies begin to decline and significant SSTA is found over the tropical Atlantic. The significant SSTA over the East Coast of America and the tropical Atlantic can persist to the end of the summer and spring, respectively. The long-persisting SSTA over the two areas may heat the free atmosphere over the global tropics, warming the troposphere over the TIO in boreal summer.

Compared with the TIO SST, the remote oceanic forcing contributes more to the enhancement of the TIO–SAH relationship in the ECHAM5 simulations. The CCs between the simulated tropospheric temperature over the TIO and the observational TIO SST in both the IOC and IOR experiments are given in Fig. 13. In the IOR experiment (the atmosphere is forced by historical SST only in the Indian Ocean), the CC is 0.52 during PRE and 0.71 during POST. The increase in CC is less than that in the IOC experiment.

#### b. The time of the abrupt shifts

The above mainly discusses the strengthening of the TIO's influence on the SAH and reveals the possible reasons in the view of the tropospheric temperature

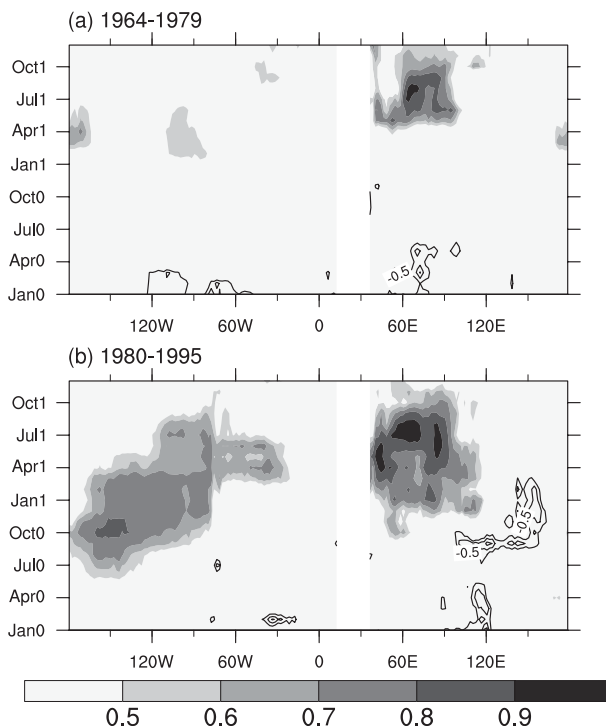


FIG. 14. Longitude–time section of correlation of the TIO SST with SSTA ( $20^{\circ}\text{S}$ – $20^{\circ}\text{N}$  mean), showing the results for (a) 1964–79 and (b) 1980–95. Shading denotes CCs for 0.5, 0.6, 0.7, 0.8, and 0.9, and contours denote those for 0.5, 0.6, 0.7, 0.8, and 0.9. Numerals “0” and “1” on the y axis denote the previous year and the year when there is basin warming in the TIO, respectively.

responses in large scale. However, mismatch exists in the time of the abrupt shifts of the TIO–SAH correlation in observation and simulations. The time is around 1976 in observation (Fig. 3) and about 1979 in simulations (Fig. 5). Some other processes independent of SST forcing may exert influences on the SAH. The processes cannot be present in the ensemble mean results. Which processes contribute to the relative lag of the shift time in the simulations are unknown and need further investigation.

## 7. Summary

Our analysis of HadISST and the NCEP–NCAR reanalysis reveals that the TIO's influence on the SAH intensity experiences a decadal shift. Before the late 1970s, the influence is weak. After the late 1970s, the influence is significant. The tropospheric temperature response appears to be responsible for the strengthening of the TIO's influence on the SAH. During the two epochs, the local tropospheric temperature responses to the TIO warming are distinct—the response is more significant during the second epoch.

Ensemble simulations of AGCMs driven by historical SST reproduce well the intensified TIO's influence on the SAH. Encouragingly, both AGCMs accurately capture the year when their relationship became significant. During the two epochs, the tropospheric temperature responses are also well reproduced. Also, most of the members (34 members out of 38) capture the strengthening of the TIO's influence on the SAH. The AGCM results indicate that the decadal change in the influence is attributed to the SST forcing.

Furthermore, the possible reasons leading to the distinct responses of the tropospheric temperature are given as follows:

- The locations of the SSTA in the TIO. During 1964–79, the significant SSTA was located in the southeastern Indian Ocean, outside of the Indian Ocean warm pool. As the background convection is weak there, the TIO warming-related SSTA do not pose a large influence on the tropospheric temperature. In contrast, because of the strengthening of the ENSO variability and thermocline shoaling in the tropical southwestern Indian Ocean during the second epoch, the TIO warming is closely associated with the northern Indian Ocean warming. The warming is located in the warm pool. Through the background vigorous convection, the SSTA can affect the above tropospheric temperature and thus the SAH. ECHAM5 simulations confirm the effect of the northern Indian Ocean SST.
- The decadal change in the mean SST and its variability. During the decades, the summertime TIO SST exhibits a significant warming trend. Combined with the strengthened SST variability, the influence of the SSTA on the atmosphere is larger after the late 1970s. Though a similar warming with increased SST variability occurs in some parts of the Atlantic and Southern Oceans, the warmer background SST may make the TIO influence the atmosphere more.

In addition, the remote oceanic forcing is discussed. The ECHAM5 simulation shows that during the second epoch, the SST over the remote oceans may favor the strengthening of the TIO–SAH relationship. From the first to the second epoch, the model results imply that the role, which the remote oceanic forcing plays in the strengthening of the TIO–SAH relationship, cannot be neglected. The detailed processes are sophisticated and require further investigation.

*Acknowledgments.* The authors wish to thank Prof. Renguang Wu, Prof. Shang-Ping Xie, and an anonymous reviewer for their insightful comments, which lead to a significant improvement in the manuscript. The study was supported by National Basic Research

Program of China (973 Program) Grants 2012CB955604 and 2011CB309704; the Third Institute of Oceanography, State Oceanic Administration Grant GCMAC1007; and the Special Scientific Research Project for Public Interest Grant GYHY201006021 and the NSFC Grant 40890155/D0601.

## REFERENCES

- Annamalai, H., P. Liu, and S. P. Xie, 2005: Southwest Indian Ocean SST variability: Its local effect and remote influence on Asian monsoons. *J. Climate*, **18**, 4150–4167.
- Boos, W. R., and Z. Kuang, 2010: Dominant control of the South Asian monsoon by orographic insulation versus plateau heating. *Nature*, **463**, 218–222.
- Charney, J. G., 1963: A note on large-scale motions in the tropics. *J. Atmos. Sci.*, **20**, 607–608.
- Chiang, J. C. H., and A. H. Sobel, 2002: Tropical tropospheric temperature variations caused by ENSO and their influence on the remote tropical climate. *J. Climate*, **15**, 2616–2631.
- Collins, W. D., and Coauthors, 2004: Description of the NCAR Community Atmosphere Model (CAM 3.0). NCAR Tech. Note NCAR/TN+464-STR, 210 pp.
- Dethof, A., A. O'Neill, J. M. Slingo, and H. G. J. Smit, 1999: A mechanism for moistening the lower stratosphere involving the Asian summer monsoon. *Quart. J. Roy. Meteor. Soc.*, **125**, 1079–1106.
- Du, Y., and S.-P. Xie, 2008: Role of atmospheric adjustments in the tropical Indian Ocean warming during the 20th century in climate models. *Geophys. Res. Lett.*, **35**, L08712, doi:10.1029/2008GL033631.
- , —, G. Huang, and K. Hu, 2009: Role of air–sea interaction in the long persistence of El Niño–induced north Indian Ocean warming. *J. Climate*, **22**, 2023–2038.
- Duan, A. M., and G. X. Wu, 2005: Role of the Tibetan Plateau thermal forcing in the summer climate patterns over subtropical Asia. *Climate Dyn.*, **24**, 793–807.
- Emanuel, K. A., J. D. Neelin, and C. S. Bretherton, 1994: On large-scale circulations in convecting atmospheres. *Quart. J. Roy. Meteor. Soc.*, **120**, 1111–1143.
- , —, and —, 1997: Reply to comments by Bjorn Stevens, David A. Randall, Xin Lin and Michael T. Montgomery on 'On large-scale circulations in convecting atmospheres.' *Quart. J. Roy. Meteor. Soc.*, **123**, 1779–1782.
- Flohn, H., 1960: Recent investigations on the mechanism of the "summer monsoon" of southern and eastern Asia. *Symposium on Monsoons of the World*, Hind Union Press, 75–88.
- Gill, A. E., 1980: Some simple solutions for heat-induced tropical circulation. *Quart. J. Roy. Meteor. Soc.*, **106**, 447–462.
- Hoskins, B. J., and M. J. Rodwell, 1995: A model of the Asian summer monsoon. Part I: The global scale. *J. Atmos. Sci.*, **52**, 1329–1329.
- Hu, K., G. Huang, and R. Huang, 2011a: The impact of tropical Indian Ocean variability on summer surface air temperature in China. *J. Climate*, **24**, 5365–5377.
- , —, X. Qu, and R. Huang, 2011b: The impact of Indian Ocean variability on high temperature extremes across southern Yangtze River valley in late summer. *Adv. Atmos. Sci.*, **29**, 91–100.

- Huang, B., and J. L. Kinter III, 2002: Interannual variability in the tropical Indian Ocean. *Geophys. Res. Lett.*, **107**, 3199, doi:10.1029/2001JC001278.
- Huang, G., K. Hu, and S. P. Xie, 2010: Strengthening of tropical Indian Ocean teleconnection to the northwest Pacific since the mid-1970s: An atmospheric GCM study. *J. Climate*, **23**, 5294–5304.
- , X. Qu, and K. Hu, 2011: The impact of the tropical Indian Ocean on the South Asian high in boreal summer. *Adv. Atmos. Sci.*, **28**, 421–432.
- Huang, R., and Y. Wu, 1989: The influence of ENSO on the summer climate change in China and its mechanism. *Adv. Atmos. Sci.*, **6**, 21–32.
- , and F. Sun, 1992: Impact of the tropical western Pacific on the East Asian summer monsoon. *J. Meteor. Soc. Japan*, **70**, 243–256.
- , G. Huang, and B. Ren, 1999: Advances and problems needed for further investigation in the studies of the East Asian summer monsoon. *Chin. J. Atmos. Sci.*, **23**, 129–141.
- Jiang, X., Y. Li, S. Yang, and R. Wu, 2011: Interannual and interdecadal variations of the South Asian and western Pacific subtropical highs and their relationship with the Asian-Pacific summer climate. *Meteor. Atmos. Phys.*, **113**, 171–180.
- Kalnay, E., and Coauthors, 1996: The NCEP/NCAR 40-Year Reanalysis Project. *Bull. Amer. Meteor. Soc.*, **77**, 437–471.
- Klein, S. A., B. J. Soden, and N.-C. Lau, 1999: Remote sea surface temperature variations during ENSO: Evidence for a tropical atmospheric bridge. *J. Climate*, **12**, 917–932.
- Li, Q., and Coauthors, 2005: Convective outflow of South Asian pollution: A global CTM simulation compared with EOS MLS observations. *Geophys. Res. Lett.*, **32**, L14826, doi:10.1029/2005GL022762.
- Mason, R. B., and C. E. Anderson, 1963: The development and decay of the 100-mb. summertime anticyclone over southern Asia. *Mon. Wea. Rev.*, **91**, 3–12.
- Matsuno, T., 1966: Quasi-geostrophic motions in the equatorial area. *J. Meteor. Soc. Japan*, **44**, 25–43.
- Park, M., W. J. Randel, D. E. Kinnison, R. R. Garcia, and W. Choi, 2004: Seasonal variation of methane, water vapor, and nitrogen oxides near the tropopause: Satellite observations and model simulations. *J. Geophys. Res.*, **109**, D03302, doi:10.1029/2003JD003706.
- Randel, W. J., and M. Park, 2006: Deep convective influence on the Asian summer monsoon anticyclone and associated tracer variability observed with Atmospheric Infrared Sounder (AIRS). *J. Geophys. Res.*, **111**, D12314, doi:10.1029/2005JD006490.
- Rayner, N. A., P. Brohan, D. E. Parker, C. K. Folland, J. J. Kennedy, M. Vanicek, T. J. Ansell, and S. F. B. Tett, 2006: Improved analyses of changes and uncertainties in sea surface temperature measured in situ since the mid-nineteenth century: The HadSST2 dataset. *J. Climate*, **19**, 446–469.
- Roeckner, E., and Coauthors, 2003: The atmospheric general circulation model ECHAM5. Part I: Model description. Max-Planck-Institut für Meteorologie Rep. 349, 140 pp.
- Sobel, A. H., and C. S. Bretherton, 2000: Modeling tropical precipitation in a single column. *J. Climate*, **13**, 4378–4392.
- Tao, S.-Y., and F. K. Zhu, 1964: The variation of 100mb circulation over South Asia in summer and its association with march and withdraw of west Pacific subtropical high. *Acta Meteor. Sin.*, **34**, 385–395.
- , and L.-X. Chen, 1987: A review of recent research on the East Asian summer monsoon in China. *Monsoon Meteorology*, C.-P. Chang and T. N. Krishnamurti, Eds., Oxford University Press, 60–92.
- Wallace, J. M., 1992: Effect of deep convection on the regulation of tropical sea surface temperature. *Nature*, **357**, 230–231.
- Wu, R., and L. Chen, 1998: Decadal variation of summer rainfall in the Yangtze-huaihe River valley and its relationship to atmospheric circulation anomalies over East Asia and western North Pacific. *Adv. Atmos. Sci.*, **15**, 510–522.
- , and S.-W. Yeh, 2010: A further study of the tropical Indian Ocean asymmetric mode in boreal spring. *J. Geophys. Res.*, **115**, D08101, doi:10.1029/2009JD012999.
- , B. P. Kirtman, and V. Krishnamurthy, 2008: An asymmetric mode of tropical Indian Ocean rainfall variability in boreal spring. *J. Geophys. Res.*, **113**, D05104, doi:10.1029/2007JD009316.
- Xie, S.-P., H. Annamalai, F. A. Schott, and J. P. McCreary, 2002: Structure and mechanisms of south Indian Ocean climate variability. *J. Climate*, **15**, 864–878.
- , K. Hu, J. Hafner, H. Tokinaga, Y. Du, G. Huang, and T. Sampe, 2009: Indian Ocean capacitor effect on Indo-western Pacific climate during the summer following El Niño. *J. Climate*, **22**, 730–747.
- , Y. Du, G. Huang, X.-T. Zheng, H. Tokinaga, K. Hu, and Q. Liu, 2010: Decadal shift in El Niño influences on Indo-western Pacific and East Asian climate in the 1970s. *J. Climate*, **23**, 3352–3368.
- Yang, J., and Q. Liu, 2008: The “charge/discharge” roles of the basin-wide mode of the Indian Ocean SST anomaly—influence on the South Asian high in summer. *Acta Oceanol. Sin.*, **30**, 12–19.
- , —, S.-P. Xie, Z. Liu, and L. Wu, 2007: Impact of the Indian Ocean SST basin mode on the Asian summer monsoon. *Geophys. Res. Lett.*, **34**, L02708, doi:10.1029/2006GL028571.
- Zhang, C., 1993: Large-scale variability of atmospheric deep convection in relation to sea surface temperature in the tropics. *J. Climate*, **6**, 1898–1913.
- Zhang, P., S. Yang, and V. E. Kousky, 2005: South Asian high and Asian-Pacific-American climate teleconnection. *Adv. Atmos. Sci.*, **22**, 915–923.
- Zhang, Q., Y. Qian, and X. Zhang, 2000: Interannual and interdecadal variations of the South Asia high. *Chin. J. Atmos. Sci.*, **24**, 67–78.
- Zhao, P., Y. Zhu, and R. Zhang, 2007: An Asian-Pacific teleconnection in summer tropospheric temperature and associated Asian climate variability. *Climate Dyn.*, **29**, 293–303.
- , X. Zhang, Y. Li, and J. Chen, 2009: Remotely modulated tropical-North Pacific ocean-atmosphere interactions by the South Asian high. *Atmos. Res.*, **94**, 45–60.
- Zhou, N., Y. Yu, and Y. Qian, 2006: Simulation for the 100-hPa South Asian high and precipitation over East Asia with IPCC coupled GCMs. *Adv. Atmos. Sci.*, **23**, 375–390.